steel research international
www.steel-research.de

The Novel Combination of Strength and Ductility in 0.4C-7Mn-3.2Al Medium Manganese Steel by Intercritical Annealing

Chao Lv, YanHua Wang, Xingmin Huang, Lei Zhang, QinQin Fu, Min Wu, and Juan Zhang*

By altering the temperature and duration of intercritical annealing (IA), the mechanical stability of retained austenites (RAs) is intentionally regulated in newly designed cold-rolled medium manganese steel of Fe-0.4C-7Mn-3.2Al (in wt%). Consequently, a novel combination of ultimate tensile strength (UTS) and total elongation (TE) (e.g., 1118 MPa and 67%) is obtained in duplex steel, and the corresponding product of UTS and TE can reach 75 GPa%. Both twinning-induced plasticity (TWIP) and transformation-induced plasticity (TRIP) take effect step by step during deformation and are conducive to the outstanding properties.

The automotive industry has been striving to reduce the weight of vehicles to increase fuel efficiency and reduce CO_2 emission.[1,2] To achieve this, advanced high-strength steels (AHSS) have proved to be among the most promising solutions. In particular, medium manganese (e.g., 5–12 wt%Mn) steel has attracted more attention for its excellent combination of strength and ductility.[1–4] By optimizing an alloy component and microstructure, medium manganese steel exhibits a better strength–ductility balance at room temperature (ultimate tensile strength [UTS]: 980–1000 MPa; total elongation [TE]: 26%–75%).[3–5] In medium manganese steels, carbon and manganese atoms tend to partition from martensite to austenite, which can help stabilize intercritical austenite to room temperature.[6,7] Al, a ferrite stabilizer, often helps form a dual-phase structure of ferrite and austenite at high temperatures[8] and also prevents the precipitation of carbides so that carbon atoms can only be partitioned into austenite during intercritical annealing (IA). Accordingly, the strengthening mechanism and deformation behavior of medium manganese steel containing various Mn and Al contents have been intensively studied.[9,10] However, the C content of most medium manganese steel is usually less than 0.2 wt% and the detailed information about toughing mechanisms such as transformation-induced plasticity (TRIP) and twinning-induced plasticity (TWIP) during deformation is still insufficient.[11–14] The present study sheds light on the room-temperature tensile properties and deformation behaviors of Fe-0.4C-7Mn-3.2Al (in wt%) cold-rolled experimental steels after different IA treatments.

The steel investigated in the study, with a measured chemical composition of Fe-0.35C-6.90Mn-3.20Al (in wt%), was fabricated by a vacuum induction melting method, followed by hot rolling between 1150 and 880 °C, to produce 4 mm-thick sheets. The hot-rolled sheets were treated at 770 °C for 30 min and then cold rolled to about 2 mm with a reduction of 50%. Subsequently, the cold-rolled sheets were intercritically annealed at temperatures of 650, 700, 750, and 800 °C for 60 min and various durations from 3 min to 1.5 h at 750 °C, followed by water quenching to room temperature, and finally, tempered at 200 °C for 20 min and air cooled to room temperature. Tempering has proved not only to relieve the internal stress but also improve the stability of austenite.

Dog bone-shaped specimens with a gauge length of 30 mm, width of 12.5 mm, and thickness of 2 mm were machined from the cold-rolled thick sheet, with the tensile axis parallel to the rolling direction. Normal and interrupted tensile tests, stopped at different engineering strains (such as 0%, 15%, 45%, and

C. Lv, Y. H. Wang, Prof. X. Huang
Key Laboratory of Advanced Technologies of Materials
Ministry of Education
School of Materials Science and Engineering
Southwest Jiaotong University
Chengdu, Sichuan 610031, P. R. China
E-mail: xmhuang@swjtu.cn

Dr. L. Zhang
State Key Laboratory of Solidification Processing
Northwestern Polytechnical University
Xi'an 710072, P. R. China

Q. Q. Fu
Centre for Advancing Materials Performance from the Nanoscale (CAMP-Nano) & Hysitron Applied Research Centre in China (HARCC)
State Key Laboratory for Mechanical Behavior of Materials
Xi'an Jiaotong University
Xi'an 710049, P. R. China

Dr. M. Wu
College of Materials Science and Engineering
Zhejiang University of Technology
Hangzhou, Zhejiang 310014, P. R. China

Dr. J. Zhang
Applied Mechanics and Structure Safety Key Laboratory of Sichuan Province
School of Mechanics and Engineering
Southwest Jiaotong University
Chengdu 610031, P. R. China

The ORCID identification number(s) for the author(s) of this article can be found under https://doi.org/10.1002/srin.201900228.

DOI: 10.1002/srin.201900228

67% [fracture strain], corresponding to the true strains of 0, 0.31, 0.4, and 0.52, respectively), were performed at a strain rate of $10^{-3}\,s^{-1}$ at room temperature in a hydraulic machine (CMT5305). The volume fraction of retained austenite (RA) (V_{RA}, in vol%) was calculated according to the standard X-ray diffraction method (D/max-2500 PC, Rigaku, Cu Kα radiation, scan rate: 2° min^{-1}, scan step size: 0.02°)[11]. Transmission electron microscopy (TEM) experiments were carried out on samples strained at 0%, 15%, 45%, and 67% on a JEOL 2100 microscope operated on an accelerated voltage of 200 kV. TEM samples were prepared using a twin-jet technique in 10% perchloric acid +90% acetic acid solution.

Figure 1 shows the engineering stress–strain curves of the studied steel, annealed to different conditions, such as IA temperature and duration. The values of yield strength (YS), UTS, and TE are summarized in **Table 1**. The stress–strain curves exhibit the yield point elongation (YPE) phenomenon at lower IA temperatures, i.e., 650 and 700 °C, but it is absent in other temperatures. When the IA temperature increases from 750 to 800 °C, the tensile behavior shows increasing stress flow after yielding. According to the literature,[15] a higher IA temperature leads to a shorter YPE in medium manganese steel and it mainly relates to the partition of C from ferrite to austenite during IA. The stress–strain curves of annealing at 800 °C exhibit serrations, which might be related to the severe and continuous TRIP effect.

As the IA temperature increases from 650 to 800 °C, YS decreases; the UTS decreases first and then increases gradually at IA temperatures of 700 and 800 °C, whereas TE reaches its maximum of 67% at 750 °C. When the IA duration remains constant for 1 h, it is worth noting that the sample annealing at 750 °C also exhibits outstanding tensile properties with a UTS of 1118 MPa and the product of strength and elongation (PSE) of 75 GPa%, which outnumbers all those reported medium Mn duplex steels until now.[5,11–13,15,16]

The average grain size of austenite is shown in Table 1. It is shown that the average grain size of austenite also increases with elevated IA temperatures, leading to a lower YS at higher temperatures. Additionally, annealing at a high temperature such as 800 °C induces more austenite grains (Table 1), resulting in a decrease in the average C/Mn content in austenite.[17] Considering the above two factors, the stability of austenite tends to be reduced, so that a large amount of austenite undergoes a transition to martensite after yielding, bringing about unusual strain-hardening behavior.

The influences of various durations on the stress–strain curves are shown in Figure 1b. It is shown that the longer duration (<1 h) of IA results in better plasticity, i.e., 60% of TE at

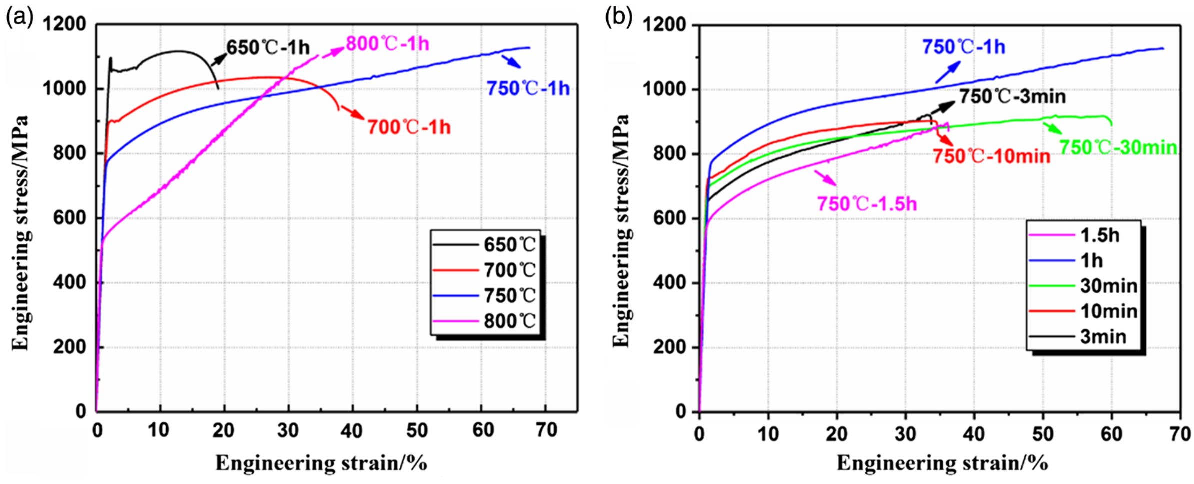

Figure 1. Engineering stress–strain curves of studied steel a) annealed at different temperatures for 1 h and b) annealed at 750 °C for various durations.

Table 1. Grain size, volume faction of RA, and tensile test results for annealed steels.

IA conditions	Grain size [μm]	Volume fraction of RA [%]	YS [MPa]	UTS [MPa]	TE [%]	UTS × TE [GPa%]
650 °C—1 h	0.50	22.2	1080	1115	19	21.2
700 °C—1 h	0.90	29.0	900	1040	38	39.5
750 °C—3 min	0.90	32.5	650	921	34	31.3
750 °C—10 min	0.98	33.5	720	930	35	32.6
750 °C—30 min	1.26	35.5	700	919	60	55.1
750 °C—1 h	1.43	33.3	780	1118	67	74.9
750 °C—1.5 h	1.76	36.0	600	897	36	32.3
800 °C—1 h	1.90	36.1	520	1157	35	40.5

30 min and 67% of TE at 1 h; however, there is a drastic decrease in both UTS and TE to 896 MPa and 36% at 1.5 h, respectively. The variation in mechanical properties herein might correlate with RA faction and stability, which is complicated due to multiple factors, such as grain size and morphology, surrounding phase, and element distribution. The relevant studies are in progress and will be published in another article.

To further understand the plasticity-enhancing mechanism of the sample annealed at 750 °C for 1 h, the corresponding relations between V_{RA} and the work-hardening rate (WHR) at the given true strain were established. As shown in **Figure 2**, the WHR curves show a multiple-stage strain-hardening behavior, where various regions are labeled as S_1, S_2, S_3, and S_4, respectively. Due to the fast-dynamic recovery of dislocations, the WHR first declined rapidly at S_1, followed by continuous reduction at S_2. In contrast, V_{RA} varies slightly in the range of 30–33 vol %, implying that only 3 vol% of RA transformed to martensite till the end of S_2. When true strain is above 0.22, the WHR first increases slightly in S_3 and strongly fluctuates in S_4, corresponding to the distinct drop of V_{RA} to 25 vol% ($\varepsilon = 0.31$) and 19 vol% ($\varepsilon = 0.4$), and finally the 17.8 vol% of RA remains in the fracture state ($\varepsilon = 0.52$). Clearly, in later stages (S_3 and S_4), the large plasticity of about 30% might be mainly attributed to about 12 vol% of RA transformation to martensite, namely the TRIP effect. As shown in Figure 2b, the WHR is characteristic of the obvious fluctuation in the S_4 stage. Li et al.[18] suppose that martensite transformation is the main reason for quick increase and abrupt drop in the $d\sigma/d\varepsilon$ curve. Li et al.[19] proposed that excellent strength and plasticity in medium Mn steel might be attributed to the discontinuous TRIP effect involving stress relaxation and transfer during deformation. As indicated in the enlarged zone of the $d\sigma/d\varepsilon$ curve, when some RA grains start to transform as fresh martensite intensively, $d\sigma/d\varepsilon$ increases quickly from P_1 (1496 MPa) to the larger value (P_2, 3462 MPa), then abruptly drops to P_3 (1302 MPa). For the next circulations, austenite with a higher degree of stability undergoes transformation at a larger true strain, leading to the sustained fluctuation of the $d\sigma/d\varepsilon$ curve in the S_4 stage. Apparently, V_{RA} reduction (1 vol%) in the true strain of 0.13–0.22 is much lower than that in later true strain (5 and 6 vol% for 0.22–0.31 and 0.31–0.40, respectively). V_{RA} reduction (about 1 vol%) is still poor in the true strain range of 0.40–0.52.

As for the earlier deformation stages, meaningful microstructure information is essentially provided in the TEM images of IA-processed steel at 750 °C for 1 h before tensile straining and at the prestrain of 15%, 45%, and 67%. As shown in **Figure 3**a,b, unstrained experimental steel has two types of austenite morphologies: block and film-like morphologies, in sizes 1–2 and 0.25 μm, respectively. For prestrained samples with a strain of 15%, deformation-induced twins were detected in RA (as shown in Figure 3c), as verified by the dark-field image and selected-area diffraction (SAD) pattern taken along the [011] zone axis of austenite. For the prestrain of 45% in the S_4 region, there are still some thick deformation twins inside the austenite grains (Figure 3e,f). Due to the partition of C and Mn from ferrite to austenite during IA, the stacking fault energy (SFE) value of some RA can increase to a proper range so that deform twinning happens.[20] When secondary twins (Figure 3g) are formed and intersect the primary twins, nucleation for the strain-induced martensite is facilitated at the intersection sites. Moreover, if dislocation pile-ups at strong barriers such as grain boundaries supply enough strain energy,[12] martensitic transformation tends to occur in regions under high resolved shear stresses, indicated by arrows in Figure 3g.[11] So, in the small true strain (<22%), the toughing mechanism of the sample should be mainly deformation twinning due to adequate austenite stability. When strain increases further, martensite transformation is subsequently motivated and WHR of the sample is enhanced.

The relationship between the UTS and TE can be expressed by the so-called banana curves for various AHSS grades. **Figure 4** summarizes the UTS and TE data of medium Mn steels in this study and in available literatures with similar Mn content levels.[3,18,19,21–28] As shown, significantly superior tensile properties could be obtained in this study. It is suggested that the newly designed medium Mn steel is a promising candidate to obtain a strength–ductility balance as high as ≈75 GPa%, which exceeds the target of ≥30–35 GPa% for the third-generation AHSS grades.

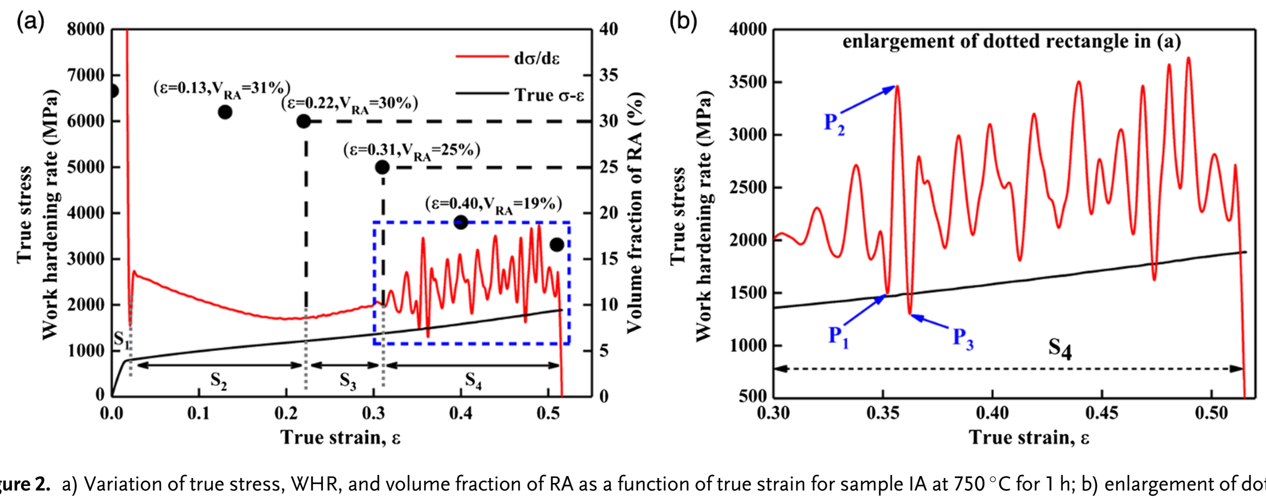

Figure 2. a) Variation of true stress, WHR, and volume fraction of RA as a function of true strain for sample IA at 750 °C for 1 h; b) enlargement of dotted rectangle in (a).

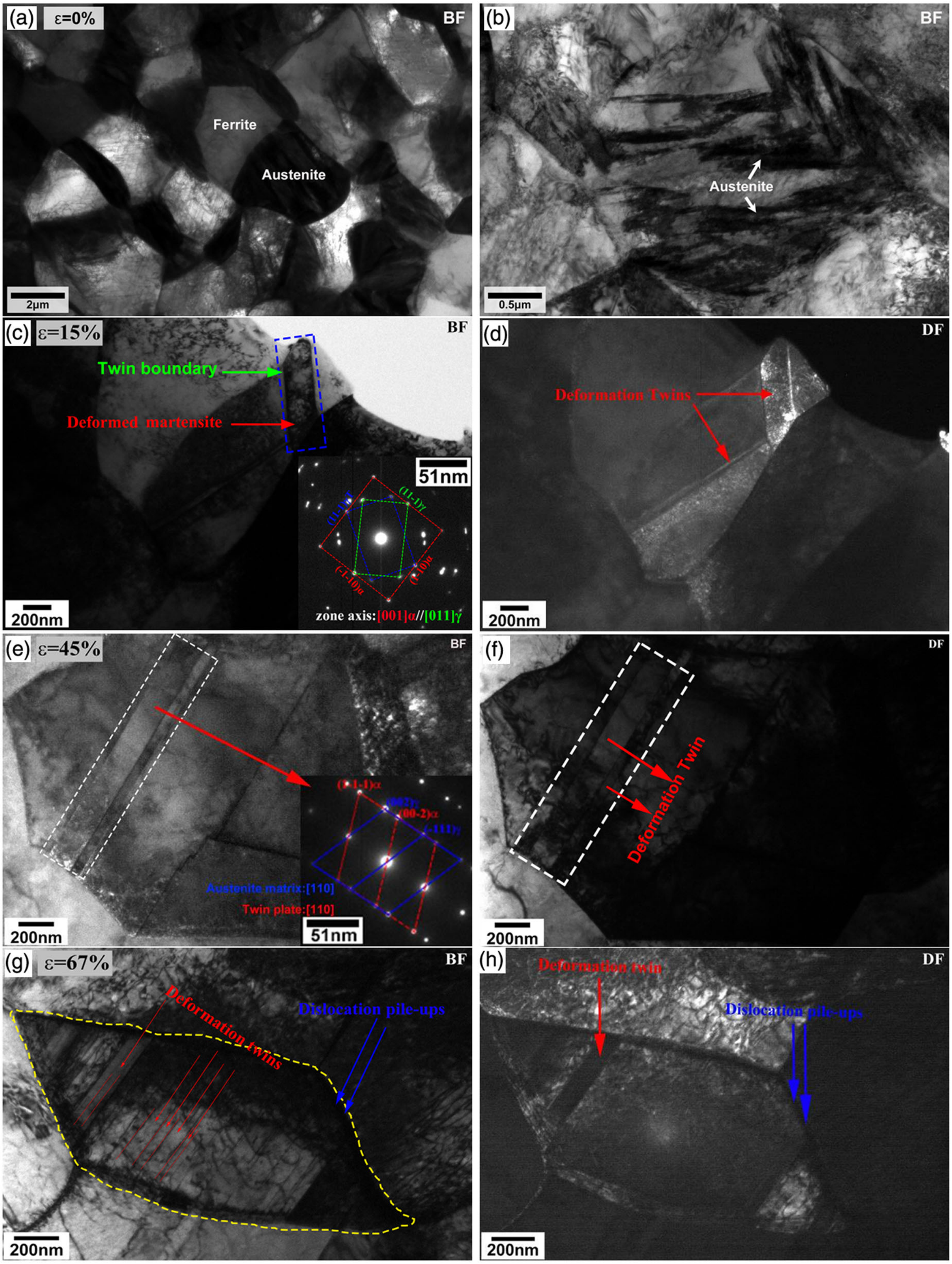

Figure 3. a,b) TEM micrographs of the microstructure of IA-processed steel at 750 °C for 1 h before tensile straining, c,d) at the strain of 15%, e,f) 45%, and g,h) 67%. a,b) Bright-field images of austenite grain at the strain of 0%, showing block and film-like austenite morphology. c,d) Bright- and dark-field images of an austenite grain (enveloped in a dotted box) at a strain of 15%, with a corresponding SAD pattern (lower right inset in (c)), showing deformation-induced twins (arrow) and twin intersections. e,f) TEM bright- and dark-field images of an austenite grain at a strain of 45%, with a corresponding SAD pattern (lower right inset in (e)), showing thick deformation-induced twins and strain-induced α′-martensite. g,h) TEM bright- and dark-field images of an austenite grain at a strain of 67% (after fracture), showing thick deformation-induced twins. The insets in (c) and (e) indicate SAD patterns of RA containing deformation-induced twins.

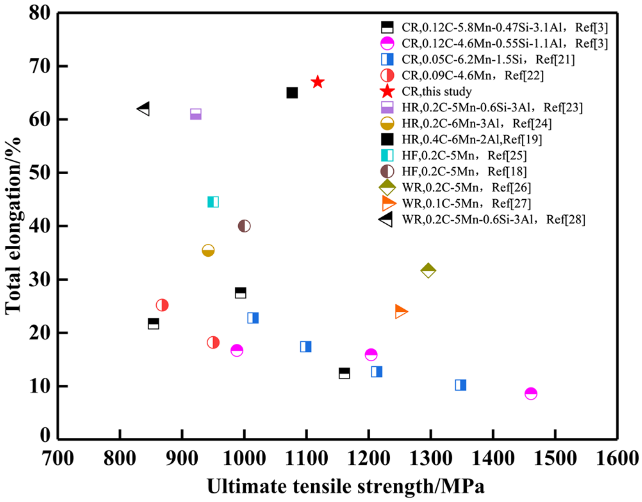

Figure 4. Dependence of TE on the UTS of the tested steels and other steels in the literature.

In summary, the present work obtained medium manganese steel with an outstanding mechanical property through IA. Both mechanical twinning and martensitic transformation were activated during deformation and made step-wise contributions to ductility. In the beginning, TWIP effect is the dominating toughing mechanism, whereas the intersection of twin might be the motivation site for martensite transformation thereafter. The considerably high stability of RA due to sufficient carbon content might postpone martensite transformation till high-level strain and stress, which finally leads to sustained TRIP effect and enhanced plasticity.

Acknowledgement

This project has no funding support.

Conflict of Interest

The authors declare no conflict of interest.

Keywords

austenite stability, intercritical annealing, medium manganese steels

Received: May 15, 2019
Revised: July 6, 2019
Published online: September 5, 2019

[1] S. Chen, R. Rana, A. Haldar, R. K. Ray, *Prog. Mater. Sci.* **2017**, *89*, 345.
[2] B. Hu, H. Luo, F. Yang, H. Dong, *J. Mater. Sci. Technol.* **2017**, *33*, 1457.
[3] D.-W. Suh, S.-J. Park, T.-H. Lee, C.-S. Oh, S.-J. Kim, *Metall. Mater. Trans. A* **2009**, *41*, 397.
[4] Z. H. Cai, H. Ding, R. D. K. Misra, Z. Y. Ying, *Acta Mater.* **2015**, *84*, 229.
[5] C.-Y. Lee, J. Jeong, J. Han, S.-J. Lee, S. Lee, Y.-K. Lee, *Acta Mater.* **2015**, *84*, 1.
[6] H. Kim, D. W. Suh, N. J. Kim, *Sci. Technol. Adv. Mater.* **2013**, *14*, 014205.
[7] S. S. Sohn, B.-J. Lee, S. Lee, J.-H. Kwak, *Met. Mater. Int.* **2015**, *21*, 43.
[8] C.-L. Lin, C.-G. Chao, J.-Y. Juang, J.-M. Yang, T.-F. Liu, *J. Alloys Compd.* **2014**, *586*, 616.
[9] Z. H. Cai, H. Ding, H. Kamoutsi, G. N. Haidemenopoulos, R. D. K. Misra, *Mater. Sci. Eng.: A* **2016**, *654*, 359.
[10] Z. H. Cai, H Ding, R. D. K. Misra, H Kong, H. Y. Wu, *Mater. Sci. Eng.: A* **2014**, *595*, 86.
[11] S. S. Sohn, K. Choi, J.-H. Kwak, N. J. Kim, S. Lee, *Acta Mater.* **2014**, *78*, 181.
[12] J. Mahieu, B. C. De Cooman, J. Maki, *Metall. Mater. Trans. A* **2002**, *33*, 2573.
[13] N. Vandijk, A. Butt, L. Zhao, J. Sietsma, S. Offerman, J. Wright, S. Van der Zwaag, *Acta Mater.* **2005**, *53*, 5439.
[14] H. Luo, J. Shi, C. Wang, W. Cao, X. Sun, H. Dong, *Acta Mater.* **2011**, *59*, 4002.
[15] H. Luo, H. Dong, M. Huang, *Mater. Des.* **2015**, *83*, 42.
[16] F. Yang, H. Luo, C. Hu, E. Pu, H. Dong, *Mater. Sci. Eng.: A* **2017**, *685*, 115.
[17] S. Lee, S. J. Lee, S. S. Kumar, K. Lee, B. C. D. Cooman, *Metall. Mater. Trans. A* **2011**, *42*, 3638.
[18] J. Li, R. Song, X. Li, N. Zhou, R. Song, *Mater. Sci. Eng.: A* **2019**, *745*, 212.
[19] Z. C. Li, H. Ding, R. D. K. Misra, Z. H. Cai, H. X. Li, *Mater. Sci. Eng.: A* **2016**, *672*, 161.
[20] S. Lee, B. C. De Cooman, *Metall. Mater. Trans. A* **2014**, *45*, 709.
[21] S. W. Lee, K. Y. Lee, B. C. De Cooman, *Mater. Sci. Forum* **2010**, *654–656*, 286.
[22] A. Arlazarov, M. Gouné, O. Bouaziz, A. Hazotte, G. Petitgand, P. Barges, *Mater. Sci. Eng.: A* **2012**, *542*, 31.
[23] C. Shao, W. Hui, Y. Zhang, X. Zhao, Y. Weng, *Mater. Sci. Eng.: A* **2017**, *682*, 45.
[24] J. Shi, X. Sun, M. Wang, W. Hui, H. Dong, W. Cao, *Scr. Mater.* **2010**, *63*, 815.
[25] H. F. Xu, J Zhao, W. Q. Cao, J Shi, C. Y. Wang, C. Wang, J. Li, H. Dong, *Mater. Sci. Eng.: A* **2012**, *532*, 435.
[26] R. Zhang, W. Q. Cao, Z. J. Peng, J. Shi, H. Dong, C. X. Huang, *Mater. Sci. Eng.: A* **2013**, *583*, 84.
[27] W. Zhan, L. Q. Cao, J. Hu, W. Q. Cao, J. Li, H. Dong, *J. Iron Steel Res. Int.* **2014**, *21*, 551.
[28] W. Hui, C. Shao, Y. Zhang, X. Zhao, Y. Weng, *Mater. Sci. Eng.: A* **2017**, *707*, 501.

